

Cite this: *Dalton Trans.*, 2016, **45**,
2261

3*H*-1,3-Azaphospholo[4,5-*b*]pyridines – novel heterocyclic P,N-bridging or hybrid ligands: synthesis and first d⁸-transition metal complexes†

Mohamed Shaker S. Adam,^{a,b} Markus K. Kindermann,^a Peter G. Jones^c and Joachim W. Heinicke^{*a}

The first 3*H*-1,3-azaphospholo-pyridines **2a–c** were synthesized as racemic mixtures in modest to medium yield by the reaction of *N*-(2-chloropyrid-3-yl)-trimethylacetimidoyl chloride **1** with RPLi₂ (R = Ph, *n*-Bu, *i*-Bu), generated from RPH₂ and BuLi in THF at –70 °C, and studied with respect to their suitability as ligands (L) in transition metal complexes. Reactions of **2a** with group 6 metal(0) pentacarbonyls led to P-coordinated LM(CO)₅ complexes **3a–5a** (Cr, Mo, W) and the reaction of **2c** with (norbornadiene)-Mo(CO)₄ surprisingly to **4c**. [Rh(1,5-COD)Cl]₂ and **2a,b**, in metal/ligand ratio 1 : 1, furnished LRh(1,5-COD)Cl complexes **6a,b** with P-coordination, **6b** accompanied by a minor contamination by the bis-coordinated L[Rh(COD)Cl]₂ complex **7b**. Reactions of **2a,b** with [(allyl)PdCl]₂ proceeded in THF with dismutation of N-coordinated (allyl)PdCl and formed with **2a** a labile crude product [(**2a**){(allyl)PdCl}_{1.2}(PdCl₂)_{0.8}]·C₄H₈O, with the composition close to L[Pd(allyl)Cl]PdCl₂ THF (**8a**·THF), which converted during crystallization to **9a**, whereas **2b** directly formed the N,N'-PdCl₂-bridged bis[LPd(allyl)chloride] complex **9b**. Conversion of **2b** with equimolar amounts of Pd(CH₃CN)₂Cl₂ in THF, or Na₂PdCl₄ in methanol, gave rise to the dimeric P,N-bridging complex **10b**. Crystal structure analyses of **6a** (*rac*), **9b**·2CDCl₃ (*meso*), **10b**·4.5THF and **10b**·2D₆-acetone (*rac*) provided detailed structural information. **10b**, but more efficiently complexes formed *in situ* from **2a,b** and Pd₂(DBA)₃ or Pd(OAc)₂, catalysed the arylamination of 2-bromopyridine with 2,4,6-trimethylaniline.

Received 16th October 2015,
Accepted 24th November 2015

DOI: 10.1039/c5dt04073f

www.rsc.org/dalton

Introduction

Various types of pyridylphosphines are known and have been applied as hybrid or hemilabile ligands in a large number of mono-, di- and polynuclear transition metal complexes and in a variety of transition-metal-catalysed organic transformations.¹ Even four-membered P,N-chelate complexes can be formed with 2-PR₂ derivatives² if the rotation of this group around the C–P bond is not hindered by a substituent in 3-position of the pyridine ring. Pyrido[*b*]-annelated phospholes or phosphinines, or partially saturated derivatives thereof with the phosphino group fixed in a ring system, are, to the best of our knowledge, still unknown except for a single 4-aza-

dibenzophosphole and a η¹P-AuCl complex of the *N*-methylated ligand.³ In connection with our investigations of pyrido[*b*]-annelated 1*H*-1,3-azaphospholes,⁴ we were interested in establishing the consequences for the coordination behaviour if the phosphorus is fixed within a cyclic structure, fused with the pyridine ring. Since the dicoordinated phosphorus of the 1*H*-1,3-azaphospholes is a weak donor and has formed isolable transition metal complexes so far only with M⁰(CO)_{*n*} fragments (M = Cr, Mo, W; *n* = 5, rarely 4 and 3)^{4,5} or, as shown for the related 1*H*-1,3-benzazaphospholes, with electron-rich d¹⁰ coinage metal compounds or HgCl₂,⁶ the first pyrido[*b*]-annelated 3*H*-1,3-azaphospholes were synthesized and tested with respect to their reactions with some transition metal compounds and as ligands in a Pd-catalysed C–N cross-coupling reaction.

Results and discussion

Ligands and LM(CO)₅ complexes

For the synthesis of the novel P,N-ligands we exploited the increased reactivity of 2-chloropyridines to electrophilic

^aInstitut für Biochemie, Ernst-Moritz-Arndt-Universität Greifswald, Felix-Hausdorff-Str. 4, 17487 Greifswald, Germany. E-mail: heinicke@uni-greifswald.de

^bDepartment of Chemistry, College of Science, King Faisal University, P.O. Box 380, Al Hufuf 31982, Al Hassa, Saudi Arabia

^cInstitut für Anorganische und Analytische Chemie, Technische Universität Braunschweig, Hagenring 30, 38106 Braunschweig, Germany

† Electronic supplementary information (ESI) available. CCDC 1423102–1423105. For ESI and crystallographic data in CIF or other electronic format see DOI: 10.1039/c5dt04073f



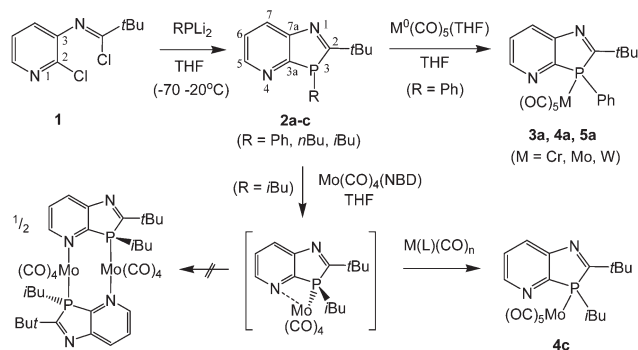
substitution compared to chlorobenzenes. The precursor *N*-(2-chloropyrid-3-yl)-imidoyl chloride **1**, accessible by refluxing *N*-(2-chloropyrid-3-yl)-pivalamide with PCl₅ in toluene, was found to react at -70 to 20 °C with RPLi₂ species (R = Ph, *n*-Bu, *i*-Bu), freshly prepared from the corresponding primary phosphines and two equivalents of *n*BuLi in THF at -70 °C, to form the *P*-substituted 1,3-azaphospholo[4,5-*b*]pyridines **2a–c** (Scheme 1). These compounds were isolated in low to moderate yields (21–59%) as oily racemic mixtures of 3*R*- and 3*S*-enantiomers. Compound **2a** solidified on storage at room temperature. The non-aromatic phosphole-type heterocycles are more sensitive to air and to decomposition by acidic OH-groups on silica gel than their aromatic 1*H*-1,3-isomers,^{4b} but vacuum distillation provided the compounds in sufficient purity for reactivity studies towards transition metal compounds.

Treatment of **2a** with M(CO)₅(THF) (M = Cr, Mo, W) in THF, prepared *in situ* by UV-irradiation of the corresponding M(CO)₆ solution, furnished at r.t. the carbonyl complexes **3a–5a** as amorphous solids in high (Cr, W) to moderate (Mo) yield. The weak CO bands at 2068, 2076 and 2075 cm⁻¹ (A₁ mode, *trans*-CO stretching) of **3a–5a** are similar or equal to the wave numbers published for the corresponding Ph₃PM(CO)₅ complexes (2065, 2074 and 2075 cm⁻¹) whereas the strong CO bands of **4a** and **5a** at 1944 and 1936 cm⁻¹ (in **3a** superimposed by the absorption of Cr(CO)₆ trace impurity) are bathochromically shifted relative to the E-bands (unsymmetric stretching of four coplanar CO ligands) of the respective Ph₃PM(CO)₅ complexes (1950 and 1942 cm⁻¹) and comparable to those of (phenyldialkylphosphine)M(CO)₅ complexes (1942 and 1937 cm⁻¹).⁷ The one-bond ³¹P–¹⁸³W coupling constant of **5a** (¹J_{PW} = 225 Hz), known to correlate in a linear fashion with the CO(_E-mode) stretching vibrations^{7a} and the total electronegativity of the *P*-substituents,⁸ even adopts a value between that of PhBu₂PW(CO)₅ and Bu₃PW(CO)₅ (¹J_{PW} = 235 and 200 Hz).^{7a} The higher donor strengths indicated by the E- than by the A₁-mode bands might be attributable to interactions between the *cis*-CO ligands and the delocalized π-system of the phosphole-type ligand, which are lacking for the perpendicularly bound *trans*-CO ligand. The ³¹P coordination chemical shifts of **3a–5a**, Δδ = 20.1, 36.8 and 60.0 ppm, are found at the

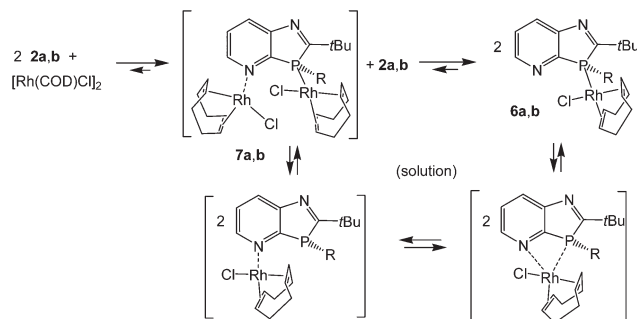
lower end of the Δδ-ranges of the M(PR₃)(CO)₅ complexes of chromium, molybdenum and tungsten.^{7a} The ¹³C NMR signals of C2 and C3a, in α-position to phosphorus, are slightly downfield-shifted by coordination of the metals at phosphorus, with a concomitant decrease of ¹J_{PC} of C2 from 35–38 in **2a–c** to 3–6 Hz (or broad singlets) in **3a–5a** but a strong increase of ¹J_{PC} of C3a from 17–20 to ca. 60–72 Hz. Coordination of M(CO)₅ at nitrogen was not observed, even if excess or two equivalents of M(CO)₅(THF) were used; this simply caused contamination by M(CO)₆. The lack of additional N-coordination is revealed by the ¹³C NMR spectra, in which a second set of *cis*-M(CO)₄ and *trans*-M(CO) signals, clearly recognizable in the spectra of the better soluble complexes **3a** and **4c**, is absent. The absence of N-coordination is further supported by minimal downfield coordination chemical shifts of C5 in **3a–5a** and **4c** (Δδ = 1.0–1.5 ppm), whereas in pyridine–W(CO)₅ complexes the Δδ values are larger, amounting to 4.9–6.3 ppm.⁹ Attempts to prepare a mono- or dimeric N,*P*-bridging complex by the reaction of **2c** (as ligand L) with an equimolar amount of Mo(NBD)(CO)₄ (NBD = norbornadiene) failed. Instead, the Mo(κ¹*P*-L)Mo(CO)₅ complex **4c** was isolated in fair yield (34%). It was unambiguously identified by its ¹³C and ³¹P NMR data (Δδ³¹P_{4c–2c} = 40.8 ppm). Whether this is attributable to the higher stability of **4c** compared to a dimeric [Mo(κ²*P,N*-L)(CO)₄]₂ complex, or to weak intramolecular interactions with the N-lone pair or π-density at the pyridine N-atom in a [Mo(L)(CO)₄] monomer, promoting dismutation reactions, was not investigated during this study.

LRh(COD)Cl complexes

Reaction of [Rh(COD)Cl]₂ in THF solution with **2a,b** in a 1 : 2 molar ratio led to cleavage of the weak μ²-chloro bridging bond (Scheme 2). The higher coordination strength at rhodium(i) of the σ³P donor compared to the imino-N-atoms, known from early measurements of reaction enthalpies of [Rh(COD)Cl]₂ with Ph₃P and pyridine¹⁰ and from the *P*-coordination in (2-PyPPh₂)Rh(COD)Cl,¹¹ led to the expected coordination at phosphorus. The racemic complexes **6a,b** were obtained in high yields as orange-yellow powders, and **6a** also as single crystals, providing detailed structural information.



Scheme 1 Synthesis of 3*H*-1,3-azaphospholo[4,5-*b*]pyridines **2a–c** and metal(0) pentacarbonyl complexes **3a–5a** and **4c**.



Scheme 2 Formation of (1,3-azaphospholo[4,5-*b*]pyridine)Rh(COD)Cl complexes **6a,b**; possible *N,P*-bis-Rh(COD)Cl intermediates **7a,b** and equilibrium species in solution.



The triclinic unit cell (space group $P\bar{1}$), contains one (*S*)- (Fig. 1) and (*R*)-enantiomer. The rhodium center is coordinated by the pyridoazaphosphole ligand through the phosphorus atom, and exhibits a distorted square-planar geometry. The Rh–P bond length is shorter than in the complexes (triarylphosphine)Rh(COD)Cl (2.297–2.3607(14) Å)^{12a} and in (*P*-*tert*-butyl-2-trimethylsilyl-1,3-benzazaphospholine)Rh(COD)Cl (2.3354(5) Å),¹³ thus implying a somewhat stronger coordination. The chloride ligand and the center of the C25–C26 double bond are arranged *cis* to phosphorus while the C21–C22 double bond is positioned *cis* to chloride. The angles of the C=C centers to the Cl- and P-atoms in the *trans*-position are effectively linear (177.5, 176.7°) and the Rh–(C=C) distance *trans* to phosphorus is 0.09 Å shorter than the Rh–(C=C) *trans* to chloride, presumably because of back bonding (*trans*-influence). Because the C3A–P3–C2 angle in the five-membered ring (87.53(4)°) is smaller than the ideal tetrahedral angle, the opposite angle Rh–P3–C11 at the distorted tetrahedral phosphorus is widened (122.16(3)°). The two imino N-atoms are far away from rhodium, both intramolecularly and also in the packing (see the ESI†), where the 3*R*- and 3*S*-enantiomers each form homochiral chains with weak intermolecular contacts (H6...Cl 2.79 and H7...Cl 2.89 Å) between the chlorine atom of the Rh(COD)Cl group and H6 and H7 of the pyridine ring of the neighbouring molecule. The chains are linked by inversion *via* the contact H19B...Cl, 2.85 Å. The intramolecular contact H20A...Cl, 2.74 Å, may also be a stabilizing factor. Both these latter contacts involve *tert*-butyl hydrogens.

The solution NMR spectra in CDCl₃ confirmed the formation of complexes **6a** and **6b** in terms of the slightly

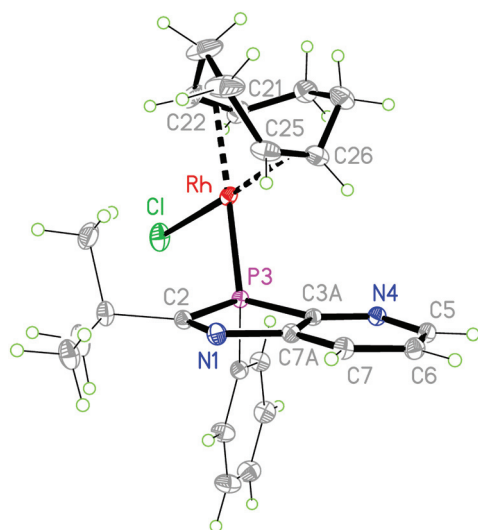


Fig. 1 Molecular structure of **6a** the (*3S*)-enantiomer is depicted; ellipsoids with 50% probability. Selected bond lengths (Å) and angles (°): Rh–P3 2.2855(3), Rh–Cl 2.3547(3), Rh–C25 2.1274(11), Rh–C26 2.1364(11), Rh–C21 2.2085(11), Rh–C22 2.2176(11), Rh–(C21=C22) 2.103, Rh–(C25=C26) 2.013, C2–P3 1.8733(10), P3–C3A 1.8144(10), N1–C2 1.2902(13), N1–C7A 1.4159(12); P3–Rh–Cl 90.624(10), C3A–P3–C2 87.53(4), C11–P3–Rh 122.16(3), N1–C2–P3 113.53(7).

reduced downfield shifts of ¹³C2 and ¹³C3a, the characteristic changes of the ¹J_{PC} coupling constants as mentioned above for **3a–5a**, and, in particular, by the downfield shifts of the phosphorus resonance ($\Delta\delta \approx 29$ ppm). The ³¹P doublets of **6a** and **6b** appear at $\delta = 27.2$ and 28.2 ppm, respectively, and thus lie within the signal range of (2-PyPPH₂)Rh(COD)Cl and (triarylphosphine)Rh(COD)Cl complexes.^{11,12} The one-bond ³¹P–¹⁰³Rh-coupling constants, ¹J_{PRh} ≈ 143 (**6a**) and 141.7 Hz (**6b**), indicative of the sum of electronegativities of the ligands at Rh(I),¹³ were smaller by *ca.* 10 Hz than in the aforementioned complexes^{11,12} and also smaller than in the aryldialkylphosphine-ligated (*P*-*tert*-butyl-1,3-benzazaphospholine)Rh(COD)Cl (¹J_{PRh} = 150.7–151.9 Hz)¹⁴ and (2-PyPiPr₂)Rh(COD)Cl complexes (¹J_{PRh} = 144.7 Hz).¹⁵ For the solution of **6a** in CDCl₃, besides the strong phosphorus doublet, a small but very broad singlet was observed at $\delta^{31}\text{P} = -1.1$ ppm (integral ratios 87–83 to 13–17%), close to that of the free ligand ($\delta^{31}\text{P} = -1.9$ ppm), which may be caused by small equilibrium amounts of N-coordinated species and/or **2a**, formed by ligand dissociation in solution. Such processes are known for the sterically hindered (*o*-Tol₃P)Rh(COD)Cl^{12a} and double exchange reactions of (Ph₃P)Rh(COD)Cl with (*p*-MeOC₆H₄)₃P-ligated LRh(CO)(acac).¹⁶ The analogous dynamic behavior of **6a** is further confirmed by rather broad aryl signals in the proton and ¹³C NMR spectra and very broad signals for the COD protons and ¹³C nuclei. An indication of involvement of pyridine nitrogen may be provided by the lack of equally intense =CH proton signals for **6a** in the range 3.1–3.6 and 5.2–5.7 ppm, typical of (triarylphosphine)Rh(COD)Cl complexes,^{11,12} and by the occurrence of a very broad signal at $\delta = 4.24$ ppm, close to the averaged =CH proton signal of (2-PyPPH₂)Rh(COD)Cl ($\delta = 4.42$ ppm).^{11,12} An averaged ¹³C signal for =CH at $\delta = 85.8$ ppm, close to that in (2-PyPPH₂)Rh(COD)Cl at $\delta = 88$ ppm and absent in (triarylphosphine)Rh(COD)Cl complexes, constitutes additional evidence in this direction. Thus, it can be assumed that the interactions with the pyridine N-atom lead in analogy to (2-PyPPH₂)Rh(COD)Cl to trigonal bipyramidal intermediates that allow rapid pseudorotation with the interchange of axial and equatorial positions and thus of the =CH nuclei in the *trans*- and *cis*-positions to phosphorus or chloride.¹¹ Coordination at the pyridine nitrogen within the ring plane and at the phosphorus of **6a** outside the ring plane disfavors intramolecular N- and P-coordination compared to pyridylphosphines, where the PR₂ group may rotate around the P–C2-bond to a suitable position and even allow P,N-chelate formation. Weak interactions with π -electrons of pyridine nitrogen, however, and thus an intramolecular Rh(COD)Cl migration, may not *a priori* be excluded, though an intermolecular mechanism of two molecules **6a** *via* an intermediate *P,N*-bis-Rh(COD)Cl complex **7a** might be a more suitable pathway. Small equilibrium amounts of **2a** might also cause similar (or further) line broadening by rapid ligand exchange reactions, long known for (Ph₃P)Rh(COD)Cl in the presence of Ph₃P.¹² Whether the imino group of the five-membered ring is also involved in solution reactions is not clear. Since the behavior of **6a** is certainly even more complicated than that of



triaryl- or pyridylphosphinorhodium complexes, a closer investigation of the dynamic behavior is a case for specialists in this field.

The solution NMR spectra of the *P*-butyl-1,3-azaphospholo-[4,5-*b*]pyridineRh(COD)Cl complex **6b** differ from those of **6a**. The proton and ^{13}C NMR signals of the olefinic =CH nuclei *trans* and *cis* to P or Cl, respectively, are not averaged out but appear in a similar region as in $(\text{Ph}_3\text{P})\text{Rh}(\text{COD})\text{Cl}^{11}$ or $(2\text{-PyPiPr}_2)\text{Rh}(\text{COD})\text{Cl}$ at low temperatures ($\leq -30^\circ\text{C}$).¹⁵ This, together with the only marginal changes in VT ^{31}P NMR spectra of **6b** in the temperature range of -56 to $+40^\circ\text{C}$, means that the ligand exchange reactions are considerably slower than in **6a** and in (2-pyridyldialkylphosphine)Rh(COD)-Cl complexes. This may be attributed to the higher complex stability of *P*-alkyl- compared to *P*-aryl-azaphospholopyridine-Rh(I) complexes and to the rigidity of the bicyclic azaphospholopyridine ligands. A small sharp ^{31}P doublet signal at $\delta = 17.2$ ppm ($J_{\text{PRh}} = 151.1$ Hz), *ca.* 5% by ^{31}P -integration, may be attributed, in accordance with the CHN values and a cationic fragment peak for $[\mathbf{7b}\text{-Cl}]^+$ in the high resolution mass spectrum, to a small amount of contamination by **7b**. N-Coordinated (pyridyl)Rh(COD)Cl complexes are known¹⁷ and thus, in addition to phosphorus of **2b**, the N-atom may also undergo coordination to the transition metal.

LPd(allyl)Cl and (LPdCl₂)₂ complexes

With the intention of ensuring complete conversion of the ligands to complexes with a 1 : 1 ligand/metal ratio, reactions of **2a** and **2b** were performed with $[\eta^3\text{-allyl}]\text{PdCl}_2$ in a molar ratio 2 : 1.5. This led in THF to orange-yellow products, soluble in THF and sparingly soluble in hexane. CHN analyses of the yellow powder, obtained from **2a** after the extraction of hexane-soluble components, were roughly consistent with a composition $[(\mathbf{2a})_2\{(\text{allyl})\text{PdCl}\}_{1.2}(\text{PdCl}_2)_{0.8}]\cdot\text{C}_4\text{H}_8\text{O}$ (close to **8a**·C₄H₈O); those of the product formed with **2b** corresponded to **9b** with a composition $[(\mathbf{2b})_2\{(\text{allyl})\text{PdCl}\}_2(\text{PdCl}_2)]$. Crystals were first obtained from a solution of the crude product formed from **2a** in THF by overlaying with hexane. These were studied by XRD and identified as complex **9a**, crystallised with THF, showing that **2a** reacts more slowly, but analogously to **2b** to form complexes of type **9**. Severe disorder of the allyl group and unexpected peaks, possibly caused by twinning, prevented satisfactory refinement. However, single crystals were then grown by slow concentration of an NMR sample of crude **9b** in CDCl₃, allowing a full and satisfactory refinement of the XRD data and unambiguous identification as **9b**·2CDCl₃ (Fig. 2).

The crystal structure analysis of **9b**·2CDCl₃ revealed an inversion-symmetric molecule in which a central PdCl₂ unit connects two $(\eta^3\text{-allyl})(\kappa^1\text{-P-azaphospholopyridine})\text{palladium}$ chloride fragments by $\kappa^1\text{N}$ -coordination within the ring plane; as a consequence of symmetry, the mutual orientation of the two pyridoazaphosphole rings is *trans* with *anti*-orientation, and the configuration at phosphorus is *R* in one and *S* in the other ring. The planes of the pyridine ring and the almost perfectly square planar N₂Pd₂Cl₂ moiety are arranged perpendicularly (interplanar angle 89.9°). The atoms Pd1, P3, Cl1,

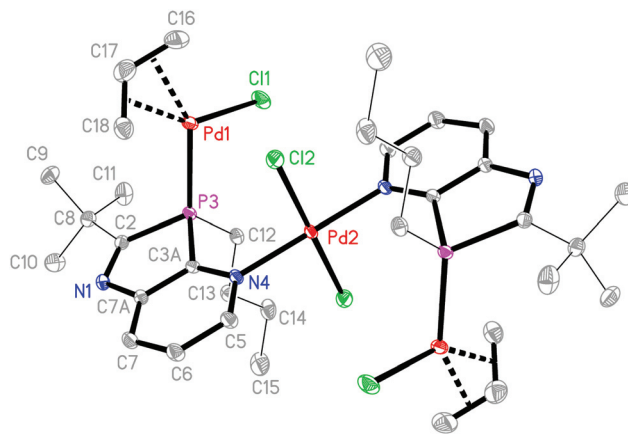


Fig. 2 Crystal structure of **9b**·2CDCl₃ (hydrogens and solvent omitted for clarity). Ellipsoids represent 50% probability levels. Selected bond lengths (Å) and angles (°): Pd1–P3 2.2685(5), Pd1–Cl1 2.3542(5), Pd1–C18 2.125(2), Pd1–C17 2.157(2), Pd1–C16 2.197(2), C16–C17 1.384(4), C17–C18 1.396(4), Pd2–N4 2.0121(15), Pd2–Cl2 2.2976(5), C2–P3 1.8506(19), P3–C3A 1.8027(18), C2–N1 1.288(2), N1–C7A 1.417(2) Å; C16–Pd1–Cl1 100.35(7), C18–Pd1–Cl1 167.66(7), C16–Pd1–P3 165.00(8), C18–Pd1–P3 97.89(7)°.

C16 and C17 are coplanar (mean deviation 0.02 Å); the angles P3–Pd1–C16 and Cl1–Pd1–C18 are roughly linear (165.00(8), 167.66(7)°). Similarly to the Rh(COD) complex **6a**, the Pd1–C16 bond length *trans* to phosphorus is shorter by 0.072 Å than the Pd1–C18 bond length *trans* to chloride. Despite this back-bonding effect, C17–C18 is still shorter than C16–C17, which suggests a slightly increased weight of a resonance structure with the C–Pd σ -bond *trans* to P and the (C=C)–Pd π -bond *trans* to the Cl atom. The P3–Pd1–Cl1 angle ($94.182(19)^\circ$) is close to the ideal 90° , but the bite angle C18–Pd1–C16 ($67.44(10)^\circ$) of the allyl group is substantially smaller and causes significant deviations of C16 and C18 from true *cis*- and *trans*-positions to Cl and P. The phosphorus atom is a distorted tetrahedral with a narrow C2–P3–C3A angle ($87.36(8)^\circ$), enforced by the five-membered azaphosphole ring, and a concomitantly increased C12–P3–Pd1 angle ($121.33(6)^\circ$). The palladium Pd1 is coordinated 2.00 Å above the mean ligand plane (average deviation 0.03 Å), and the *n*-butyl group is directed towards the opposite side, with C12 lying 1.56 Å out of the plane. In the crystal packing the molecules are connected to form ribbons parallel to [110] by weak interactions of 2.89, 2.76 Å between chlorine Cl1 of the Pd(allyl)Cl groups and H6 and H7 of the pyridine rings of the neighbouring molecules, in a fashion similar to that observed for **6a** (an intramolecular contact H5...Cl1, 2.71 Å across the inversion centre, is also observed). In addition, short N...D and Cl...Cl contacts of 2.53 and 3.49 Å respectively are observed between CDCl₃ and the molecules of **9b** (Fig. 3).

The surprising coordination of PdCl₂ as well as (allyl)PdCl may be explained by primary formation of *P*- and *N*-bis(allylPdCl) azaphospholopyridine complexes, formed by the association of the P,N-ligand with the weakly chloro-bridged



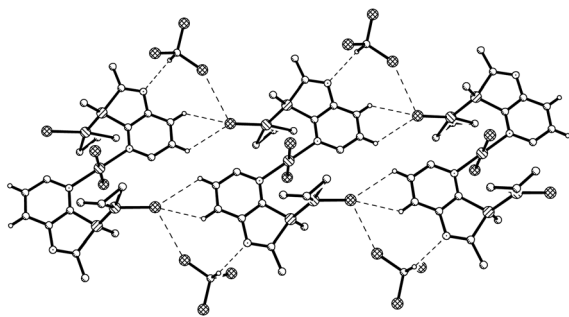
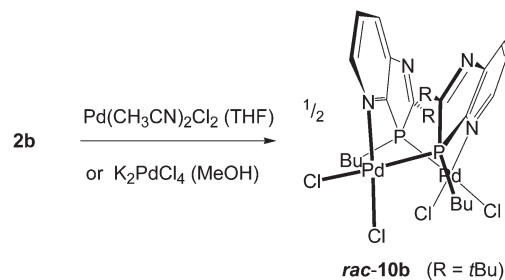


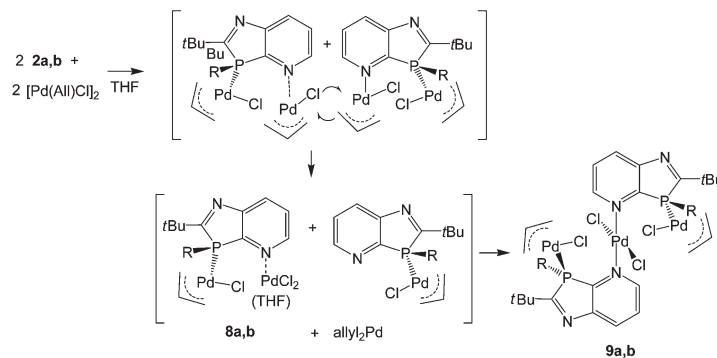
Fig. 3 Packing of **9b**·2CDCl₃ in the crystal (*n*- and *tert*-butyl groups indicated by their α -C atoms). Dashed lines represent weak C–H...Cl and C–D...N hydrogen bonds or Cl...Cl contacts.

(allylPdCl) dimer and subsequent dismutation of the less stable *N*-coordinated (allyl)PdCl fragment. Since *N*-pyridyl-Pd(allyl)Cl complexes¹⁸ have not been reported to convert to *N*-pyridyl-PdCl₂ complexes, activation of this process is assumed to be connected with the proximity of the *P*-coordinated (allyl)PdCl group. A possible scenario might be a chloro-bridging interaction, leading to a more labile penta-coordinated Pd(allyl)Cl group that could undergo allyl-chloride exchange reaction with a second molecule. This would lead to **8a**, which together with THF and a small residual amount of the primary product would be consistent with the composition of the crude product formed from **2a** and, after combination with the intermediate LRh(allyl)Cl, with the formation of **9a,b** (Scheme 3). The atomic balance of the chloro atoms in **9a,b** shows that the reaction actually proceeded in a ligand/metal ratio of 1 : 2. The assumption of an allyl-Cl exchange implies the formation of (allyl)₂Pd, removed by washing the products with hexanes on work-up. A small shoulder ($\delta = 58$ ppm) at the upfield end of the allyl ¹³CH₂ resonance ($\delta = 62.8$ ppm) in the ¹³C solution NMR spectrum of [(**2a**){(allyl)PdCl}_{1.2}(PdCl₂)_{0.8}].C₄H₈O, close to the upfield =CH₂ signal of diallylpalladium ($\delta = 54.6$ in D₈-toluene¹⁹), might be a hint at this species, formed by dismutation of the residual (**2a**)(allylPdCl)₂ complex of the crude product. The corresponding CH₂-signals of *N*- and *P*-(allyl)PdCl compounds absorb at lower field ($\delta = 61$ –63 ppm)^{18,20} and are not responsible for this shoulder.

To obtain information on the nature of palladium complexes containing only PdCl₂ units and azaphospholo[4,5-*b*]pyridines, ligand **2b** was treated with bis(acetonitrile)palladium dichloride in THF and in a second experiment with potassium tetrachloropalladate in methanol, each in a 1 : 1 molar ratio (Scheme 4). The rigidity of the aromatic pyridine ring, coordinating the metal at nitrogen within the ring plane, together with the rigid position of the tetrahedrally coordinated phosphorus in the five-membered ring with the metal outside the pyridine ring plane are inappropriate for the formation of stable mononuclear four-membered *N,P*-chelate complexes. At best, labile intermediates with some stabilization by π -interactions with the pyridine *N*-atom outside the ring plane are conceivable. These should either dimerize or polymerize to more stable products with coordination at nitrogen within the ring plane. The orange-yellow and yellow complexes, formed from the two different precursors, differed in their solubility, the first being well soluble in THF or CDCl₃, the second rather sparingly soluble in these solvents and better soluble only in more polar solvents such as methanol or acetone. The NMR spectra indicated complex formation by downfield shifts of the phosphorus resonance, $\Delta\delta = 33.5$ and 29.2 ppm, respectively, slightly (*C_q* of 2-*t*Bu) and clearly (*C7a*) increased ²*J*_{PC} coupling constants, typically for complexes of **2b**, and a somewhat downfield shifted 2-*t*Bu proton singlet, while the majority of the ¹³C and proton signals is scarcely



Scheme 4 Formation of dimeric (1,3-azaphospholopyridine- κ^1P , κ^1N)-PdCl₂ complexes **10b** with schematic presentation of its “twisted boat structure”.



Scheme 3 Reaction of **2a,b** with [η^3 -(allyl)PdCl]₂ via assumed intermediates **8a,b** to **9a,b**.

changed by the coordination. However, XRD analyses of crystals of both products, grown by slow diffusion of hexane into the complex solution in THF or by slow concentration of the D₆-acetone solution, respectively, revealed in both cases a dimeric structure consisting of $[cis\text{-Cl}_2\text{Pd}(\text{L-P},\text{N}')]_2$ moieties with Pd(II) bound at P and pyridine-N' or P' and pyridine-N, one from each azaphospholopyridine bridging ligand. Both structures exhibit the two ligands on the same side (*syn*-form) of the connecting Cl–Pd–P axes with opposite orientation of the five- and six-membered rings, so that they are different solvates of the same dinuclear complex **10b**. Neither complex displays imposed crystallographic symmetry, but the THF solvate has approximately twofold symmetry (r.m.s. deviation 0.04 Å), while the acetone solvate does not, because of different orientations of the substituents. The ligand ring systems remain planar (mean deviations 0.01–0.02 Å) and the interplanar angles are 32° and 27° respectively for the THF and acetone solvates. The square planar configuration around Pd(II), with *cis*-orientation of the two chloride ligands, causes an almost perpendicular orientation of the Cl–Pd–P axis towards the plane of the N-coordinated pyridine ring (angles between Cl...P vector and normal to the ligand plane 87–89°), while the coordination of the distorted tetrahedral phosphorus outside the pyridine-ring plane of the respective ligand enforces a considerable mutual twisting of the N–Pd–Cl axes of the two Cl₂PdNP fragments in the dimer (angle between vectors N4'...Cl1 and N4...Cl3: 62, 61°) and a “twisted boat structure” for the central eight-membered ring. The mutual orientation of the two azaphospholopyridine ligands, together with the local twofold symmetry, implies the same configuration for the two P atoms in the dimers and leads for both **10b**-4.5THF and **10b**-2D₆-acetone (Fig. 4), to pairs of (3*S*,3'*S*)- and (3*R*,3'*R*)-diastereoisomers, co-crystallising as racemic products. Different packing in the crystals of **10b**-4.5THF and **10b**-2D₆-acetone must thus be caused by the different solvent molecules; the large number of H...Cl and H...O contacts however makes an exact analysis difficult. The Pd–P, Pd–N and Pd–Cl and intra-ligand bond lengths and angles exhibit no special features and are similar in both complexes and also in (*R,S*)-**9b**-2CDCl₃. The somewhat longer Pd–Cl bond *trans* to phosphorus compared to that *trans* to nitrogen reflects the known stronger *trans* influence of P *versus* N donors.

Catalytic tests

Pyridylphosphines¹ have found wide applications in transition-metal-catalysed organic syntheses. The hemilabile properties, known also from other P,N ligands,²¹ might be advantageous by enabling temporary substrate binding on replacement of the more labile donor and catalyst stabilization after reductive elimination by re-occupation of an empty coordination site. For the first test of the suitability of azaphospholopyridine complexes as catalysts the known *N*-arylation of 2,4,6-trimethylaniline (mesitylamine) with 2-bromopyridine^{22,23} was chosen, providing 2-mesitylaminopyridine (**11**) as a potential precursor for the synthesis of *N*-mesityl-substituted 1,3-azaphospholo[5,4-*b*]pyridine.^{4b} C–N cross-couplings of this

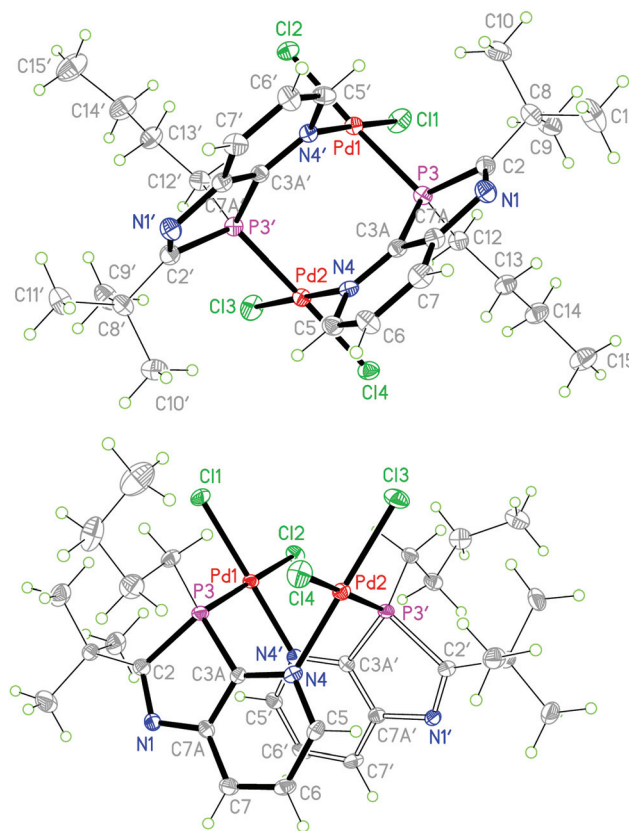
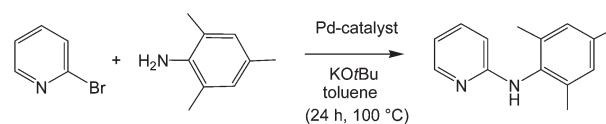


Fig. 4 (a) View of the (3*S*,3'*S*)-enantiomers in the crystal of **10b**-4.5THF (above) and (b) in the crystal of **10b**-2(D₆-acetone) (below, alternative view direction); solvents omitted for clarity, ellipsoids with 50% probability. Selected bond lengths (Å) and angles (°) for **10b**-4.5THF: Pd1–P3 2.2397(9), Pd1–N4' 2.048(3), Pd1–Cl1 2.2725(9), Pd1–Cl2 2.3396(8), C2–P3 1.865(3), P3–C3A 1.808(3), P3–C12 1.821(3); N4'–Pd1–Cl1 178.70(8), N4'–Pd1–P3 90.62(8), N4'–Pd1–Cl2 89.47(8), P3–Pd1–Cl1 88.39(3), P3–Pd1–Cl2 176.55(3), Cl1–Pd1–Cl2 91.57(3), C2–P3–C3A 87.61(15), C12–P3–Pd1 122.68(11), N1–C2–P3 113.7(2); bond lengths and angles of **10b**-2(D₆-acetone) are similar (see deposited material for details).

type, also known as Buchwald–Hartwig reactions,²⁴ are important tools for the production of arylamine fine chemicals.²⁵ The coupling according to Scheme 5 was carried out using a similar protocol to that used with the formerly applied catalysts,^{22,23} to allow a comparison of the catalytic performance. The reactants were heated in toluene in the presence of two equivalents of KO^{*t*}Bu with 5 mol% **10b** or precatalysts, prepared *in situ* from **2a** or **2b** and Pd(OAc)₂ or Pd₂DBA₃ (DBA – dibenzoylacetone) in a 1 : 1 or 2 : 1 molar ratio. With **10b** the



Scheme 5 The Pd-catalysed C–N coupling reaction of 2-bromopyridine with mesitylamine.



Table 1 Screening of **10b** and *in situ* generated azaphosphopyridine–Pd catalysts in the arylamination of 2-bromopyridine^a

Entry	Pd compound	Ligand	Metal/ligand ratio	Mol% ligand	Yield (%)
1	10b	—	1 : 1	5	26
2	Pd ₂ DBA ₃	2a	1 : 1	5	57
3	Pd ₂ DBA ₃	2a	1 : 2	10	43
4	Pd ₂ DBA ₃	2b	1 : 1	5	54
5	Pd ₂ DBA ₃	2b	1 : 2	10	42
6	Pd(OAc) ₂	2b	1 : 1	5	51
7	Pd(OAc) ₂	2b	1 : 2	10	33
8	Pd ₂ DBA ₃	Ph ₃ P	1 : 2	10	21
9	Pd ₂ DBA ₃	(<i>p</i> -Tol) ₃ P	1 : 2	10	23
10	Pd ₂ DBA ₃	(<i>o</i> -Tol) ₃ P	1 : 2	10	18

^a Reaction conditions: Heating of 2-bromopyridine, mesitylamine and KO^tBu with the given amount of **10b** or the given ligand and Pd-compound in toluene for 24 h at 100 °C; yields refer to isolated product after separation by column chromatography.

yield of **11** was rather low (Table 1, entry 1, 26%), comparable to that obtained with catalysts for comparison generated *in situ* from Pd₂DBA₃ and triphenyl- or tri-tolylphosphines (1 : 2 molar ratio), whereas the catalysts formed from **2a** or **2b** and Pd(OAc)₂ or Pd₂DBA₃ gave higher yields, particularly for a 1 : 1 molar ratio of metal to ligand (Table 1, entries 2, 4 and 6). The maximum yield of 57% (after isolation) is not high, but is higher than the reported results with DPPE/Pd₂DBA₃ (51% yield for 2 mol% catalyst and heating with 2 equiv. NaO^tBu overnight)²² and 2,3-bis(diphenyl)quinoxaline/Pd(OAc)₂ or Pd₂DBA₃ (36–43% yield with 2–5 mol% catalyst, conditions as here).²³

Conclusions and outlook

The first synthesis of 3*H*-1,3-azaphospho-pyridines, which except for a single 4-aza-dibenzophosphole seem also to be the first representative of pyrido[*b*]-annelated five- and six-membered heterocycles containing one phosphorus atom, paves the way for investigations of transition metal complexes of these novel P,N ligands, closely related to 2-pyridylphosphines, but with restricted flexibility and lacking free rotation around the C–P bond at the pyridine ring. The first examples of such complexes, hints at dynamic properties and applicability to transition-metal-catalysed reactions were presented. The asymmetry at phosphorus and the potential for a wide range of different P- and/or N-coordinated complexes, including bridging or cluster compounds as known for pyridyl phosphine ligands, open a wide field for coordination chemical studies with the novel ligands. If the additional imino donor of the five-membered ring is also involved in transition metal coordination, even a three-dimensional metal–ligand network might become accessible. Last but not least, electronic delocalization within the effectively planar imino-conjugated pyridine π -system might lead to transition metal complexes with interesting redox and/or photophysical properties.

Experimental

All manipulations were carried out under an atmosphere of dry argon or nitrogen using Schlenk techniques. Solvents were dried over sodium ketyl and distilled before use. 3-Amino-2-chloropyridine, primary phosphines and transition metal compounds were used as purchased. NMR spectra were recorded on a multinuclear FT-NMR spectrometer ARX300 or Avance300 (Bruker) at 300.1 (¹H), 75.5 (¹³C), and 121.5 (³¹P) MHz and 298 K. The ¹H, ¹³C and ³¹P chemical shifts are δ values and given in ppm relative to Me₄Si and H₃PO₄ (85%), respectively, as external standards or to solvents calibrated with the aforementioned standards. Coupling constants refer to H–H (¹H NMR) or P–C couplings (¹³C NMR) unless stated otherwise. NMR assignment numbers follow the nomenclature, and are illustrated in Scheme 1 for the compounds **1** and **2a–c** and used also for the coordinated ligands. For atom numbers in crystal structures see Fig. 1–4. Mass spectra were recorded on a single-focusing sector field mass spectrometer AMD40 (Integra, EI 70 eV); HRMS spectra were recorded on a double-focusing sector field mass spectrometer MAT 95 (Fa. Finnigan, EI 70 eV) or an ion cyclotron resonance-mass spectrometer APEX IV (Bruker Daltonik, ESI in MeOH, NH₄OAc). Elemental analyses (C, H, N) were carried out using a LECO elemental analyzer, Model CHNS-932, under standard conditions.

N-(2-Chloropyrid-3-yl)-trimethylacetimidoyl chloride (**1**)

(a) Trimethylacetylchloride (5.14 mL, 42.0 mmol) was added dropwise to a solution of 3-amino-2-chloropyridine (4.5 g, 35.0 mmol) and triethylamine (5.85 mL, 42.0 mmol) in THF (20 mL) and Et₂O (20 mL) at 0 °C. The reaction mixture was stirred for 1 h at 0 °C, overnight at room temperature, and then treated with water to remove trimethylamine hydrochloride, trimethylacetic acid and pyridinium salts. The aqueous phase was separated, extracted with ether, the combined organic phase washed with a concentrated aqueous solution of NaHCO₃, and then dried over MgSO₄. The solvent was removed in a vacuum to give 6.2 g (83%) of NMR-spectroscopically pure *N*-2-chloropyrid-3-yl-trimethylacetamide, which was used without recrystallization in step (b). ¹H NMR (CDCl₃): δ = 1.36 (s, 9 H, CMe₃), 7.27 (t, ³J = 8.2, 4.7 Hz, 1 H, H-5), 8.00 (v br, NH), 8.11 (dd, ³J = 4.7, ⁴J = 1.7 Hz, 1 H, H-6), 8.76 (dd, ³J = 8.2, ⁴J = 1.8 Hz, 1 H, H-4).

(b) Phosphorus pentachloride (5.1 g, 24.5 mmol) was added to a solution of *N*-2-chloropyrid-3-yl-trimethylacetamide (5.1 g, 24.0 mmol) in dry toluene (50 mL). The reaction mixture was refluxed for 4 h, after which the solvent and volatile by-products were removed under vacuum. The residue was distilled at 10^{−5} mbar/96 °C to give 5.0 g (90%) of **1** as colourless oil. ¹H NMR (CDCl₃): δ = 1.30 (s, 9 H, CMe₃), 7.08 (dd, ³J = 7.8, ⁴J = 1.6 Hz, 1 H, H-4), 7.14 (dd, ³J = 7.8, 4.8 Hz, 1 H, H-5), 8.08 (dd, ³J = 4.8, ⁴J = 1.6 Hz, 1 H, H-6). ¹³C{¹H} NMR (CDCl₃): δ = 27.90 (CMe₃), 43.97 (CMe₃), 122.57 (C-5), 129.06 (C-4), 141.38, 141.49 (C_q-2, C_q-3), 144.70 (C-6), 160.48 (C=N). MS (EI 70 eV, 65 °C): *m/z* (%) = 232 (5), 230 (8) [M⁺], 197 (21), 195 (66), 141 (28),



139 (84), 57 (100). Anal. calcd for C₁₀H₁₂Cl₂N₂ (231.12): C 51.97, H 5.23, N 12.12; found: C 51.87, H 5.38, N 12.00.

DL-(2-*tert*-Butyl-3-phenyl-1,3-azaphospholo[4,5-*b*]pyridine (2a)

n-Butyl lithium solution (19.4 mL, 1.6 M in hexane, 31.4 mmol) was slowly added while stirring at -70 °C to phenylphosphine (1.70 mL, 15.44 mmol) dissolved in THF (20 mL). After 1 h a solution of **1** (2.90 g, 12.6 mmol) in THF (100 mL) was added dropwise at -70 °C to the reaction mixture. Stirring was continued for 1 h at low temperature and then overnight at room temperature. The solvent was removed under vacuum, the residue was extracted with Et₂O (50 mL), and ether was evaporated. The residue was distilled at 10^{-5} mbar/95–100 °C (bath temp.) to give 0.71 g (21%) pale yellow oily **2a**, which solidified on storage at room temperature. ¹H NMR (CDCl₃): δ = 1.27 (s, 9 H, CMe₃), 7.20–7.38 (m, 6 H, phenyl, H-6), 8.05 (ddd, ³J = 8.1, ⁴J = 1.3, ⁴J_{PH} = 1.7 Hz, 1 H, H-7), 8.48 (dt, ³J = 4.8, ⁴J = 1.3, ⁴J_{PH} = 1.2 Hz, 1 H, H-5). ¹³C{¹H} NMR (CDCl₃): δ = 30.09 (d, ³J = 5.3 Hz, CMe₃), 40.65 (d, ²J = 16.7 Hz, CMe₃), 123.17 (s, C-6), 128.86 (d, ¹J = 13.3 Hz, C_q-i), 129.10 (d, ³J = 9.2 Hz, 2 C-*m*), 129.45 (s, C-7) 130.46 (d, ⁴J = 1.9 Hz, C-*p*), 135.02 (d, ²J = 20.6 Hz, 2 C-*o*), 147.61 (d, ³J = 9.9 Hz, C-5), 151.93 (d, ²J = 18.9 Hz, C_q-7a), 164.68 (d, ¹J = 20.3 Hz, C_q-3a), 200.64 (d, ¹J = 35.1 Hz, C_q-2). ³¹P{¹H} NMR: δ = -1.9 (CDCl₃); -4.4 (D₆-DMSO). MS (EI 70 eV, 25 °C): *m/z* (%) = 269 (17), 268 (100) [M⁺], 253 (71), 212 (45), 211 (30), 139 (34), 57 (88). HRMS (EI, 70 eV): calcd for [M]⁺ 268.1124; found: 268.1128. Anal. calcd for C₁₆H₁₇N₂P (268.29): H 6.39, N 10.44; found: H 6.16, N 10.27.

DL-(3-*n*-Butyl-2-*tert*-butyl-1,3-azaphospholo[4,5-*b*]pyridine (2b)

Compound **2b** was prepared in analogy to **2a** by lithiation of *n*-butylphosphine (1.47 mL, 13.1 mmol) in THF (10 mL) at -70 °C with *n*-butyl lithium (16.4 mL, 1.6 M in hexane, 26.16 mmol), and subsequent reaction with a solution of **1** (2.52 g, 10.9 mmol) in THF (80 mL) at -70 °C to room temperature and work-up as described above to give 1.6 g (59%) of an air sensitive pale yellow viscous oil, distilled at 10^{-5} mbar/90–96 °C (bath). ¹H NMR (CDCl₃): δ = 0.72 (t, ³J = 7.0 Hz, 3 H, CH₃), 1.05–1.32 (m, 6 H, CH₂), 1.34 (s, 9 H, CMe₃), 7.21 (dd, ³J = 8.1, 4.8 Hz, 1 H, H-6), 7.91 (dt, ³J = 8.1, ⁴J = 1.3, ⁴J_{PH} = 1.6 Hz, 1 H, H-7), 8.43 (dt, ³J = 4.8, ⁴J \approx ⁴J_{PH} = 1.2, 1.3 Hz, 1 H, H-5). ¹³C{¹H} NMR (CDCl₃): δ = 13.10 (s, Me), 23.47 (d, *J* = 8.0 Hz, CH₂), 24.92 (d, *J* = 20.2 Hz, CH₂), 28.40 (d, *J* = 1.5 Hz, CH₂), 29.32 (d, ³J = 4.8 Hz, CMe₃), 39.74 (d, ²J = 17.2 Hz, CMe₃), 122.19 (s, C-6), 128.68 (s, C-7), 146.57 (d, ³J = 9.7 Hz, C-5), 151.13 (d, ²J = 17.5 Hz, C_q-7a), 163.38 (d, ¹J = 17.2 Hz, C_q-3a), 200.13 (d, ¹J = 38.3 Hz, C_q-2). ³¹P{¹H} NMR (CDCl₃): δ = -2.5 . MS (EI 70 eV, 20 °C): *m/z* (%) = 249 (2), 248 (26) [M⁺], 192 (35), 191 (100) [M – Bu⁺], 165 (48), 149 (28), 148 (29), 137 (21), 136 (29), 57 (35). HRMS (ESI in MeOH, NH₄OAc): C₁₄H₂₁N₂P (248.30) calcd for [M + H]⁺ 249.15151; found 249.15161.

DL-(2-*tert*-Butyl-3-isobutyl-1,3-azaphospholo[4,5-*b*]pyridine (2c)

Compound **2c** was prepared in analogy to **2a** by lithiation of isobutylphosphine (0.70 mL, 6.22 mmol) in THF (10 mL) at

-70 °C with *n*-butyl lithium (7.81 mL, 1.6 M, 12.5 mmol), reaction with a solution of **1** (1.20 g, 5.19 mmol) in THF (80 mL) at -70 °C to room temperature and work-up as described above to give at 10^{-5} mbar/80–85 °C (bath) 0.81 g (33%) air sensitive slightly contaminated pale yellow oily **2c**. ¹H NMR (C₆D₆): δ = 0.75–1.0 (m, 6 H, CHMe_{AB}), 1.37 (s, 9 H, CMe₃), 1.6–2.05 (br m, 2 H, PCH₂), 2.10–2.30 (m, 1 H, CH), 6.72 (dd, ³J = 8.0, 4.8 Hz, 1 H, H-6), 7.83 (dt, ³J = 8.0, ⁴J = ⁴J_{PH} = 1.5 Hz, 1 H, H-7), 8.40 (ddd, ³J = 4.8, ⁴J = 1.5, ⁴J_{PH} = 1.0 Hz, 1 H, H-5). ¹³C{¹H} (CH-COSY, DEPT135) NMR (C₆D₆): δ = 24.38 (d, ³J = 7.3 Hz, CMe_A), 24.67 (d, ³J = 8.4 Hz, CMe_B), 28.17 (d, ²J = 9.0 Hz, CH), 30.79 (d, ³J = 5.1 Hz, CMe₃), 35.72 (d, ¹J = 19.3 Hz, PCH₂), 40.98 (d, ²J = 17.3 Hz, CMe₃), 123.33 (s, CH-6), 129.90 (s, CH-7), 147.79 (d, ³J = 10.0 Hz, CH-5), 152.26 (d, ¹J = 18.6 Hz, C_q-3a), 166.17 (d, ²J = 17.4 Hz, C_q-7a), 201.48 (d, ¹J = 37.8 Hz, C_q-2). ³¹P{¹H} NMR (C₆D₆): δ = -10.2 . MS (EI 70 eV, 250 °C): *m/z* (%) = 249 (8), 248 (31) [M⁺], 192 (62), 191 (89), 177 (100). HRMS (ESI in MeOH/NH₄OAc): C₁₄H₂₁N₂P (248.30), calcd for [M + H]⁺ 249.15151, found: 249.15160.

DL-(2-*tert*-Butyl-3-phenyl-1,3-azaphospholo[4,5-*b*]pyridine- κ^1 P)-pentacarbonyl chromium(0) (3a)

A solution of Cr(CO)₅(THF), prepared by irradiation of Cr(CO)₆ (351 mg, 1.60 mmol) in THF (30 mL; 36 mL of CO evolved), was added to a solution of **2a** (214 mg, 0.797 mmol) in THF (10 mL) at -10 °C. The solution was warmed to room temperature and stirred for 2 d. The solvent was evaporated under vacuum, excess Cr(CO)₆ was removed under high vacuum, and the residue was extracted with ether/hexane yielding 330 mg of an air-sensitive pale brown powder with rather low solubility, still containing some Cr(CO)₆. ¹H NMR (CDCl₃): δ = 1.31 (s, 9 H, CMe₃), 7.37–7.51 (m, 6 H, phenyl and H-6), 8.07 (ddd, ³J = 8.1, ⁴J_{PH} = 2.4, ⁴J = 1.2 Hz, 1 H, H-7), 8.63 (dd, ³J = 4.3, ⁴J \approx 1 Hz, 1 H, H-5). ¹³C{¹H} NMR (CDCl₃): δ = 30.10 (d, ³J = 2.3 Hz, CMe₃), 41.03 (d, ²J = 18.0 Hz, CMe₃), 125.05 (C-6), 129.43 (d, ³J = 10.6 Hz, 2 C-*m*), 131.7, 131.8 (C-7, C-*p*), 133.15 (d, ²J = 12.0 Hz, 2 C-*o*), 149.09 (d, ³J = 14.2 Hz, C-5), 215.53 (d, ²J = 11.9 Hz, 4 *cis*-CO); C_q signals except for *cis*-CO at the noise level. ³¹P{¹H} NMR (CDCl₃): δ = 58.1. MS (EI 70 eV, 90 °C): *m/z* (%) = 460 (4), 349 (5), 348 (20) [M⁺ – 4CO], 321 (22), 320 (100) [M⁺ – 5CO], 52 (98) [Cr⁺]. HRMS (ESI in MeOH + NH₄OAc): C₂₁H₁₇CrN₂O₅P (460.34) calcd for: [M + H]⁺ 461.03530, found: 461.03530. IR (KBr): ν (CO) = 2068 (w) cm⁻¹; the very strong band at 1950 cm⁻¹ is superimposed by the absorption of the Cr(CO)₆ contamination.

Detection of DL-(2-*tert*-butyl-3-phenyl-1,3-azaphospholo[4,5-*b*]pyridine- κ^1 P)pentacarbonyl molybdenum(0) (4a)

A solution of Mo(CO)₅(THF), prepared by irradiation of Mo(CO)₆ (208 mg, 0.79 mmol) in THF (20 mL; 18 mL of CO evolved), was added to a solution of **2a** (141 mg, 0.53 mmol) in THF (5 mL) at -10 °C. Filtration, removal of the solvent after 2 d at room temperature and repeated extraction of unconverted **2a** from the crude product with ether/hexane afforded 105 mg (40%) of an air-sensitive pale brown powder with rather low solubility. ¹H NMR (D₆-acetone): δ = 1.33 (s, 9 H, CMe₃),



7.46–7.64 (m, 6 H, phenyl and H-6), 8.19 (ddd, $^3J = 8.0$, $^4J_{\text{PH}} = 2.6$, $^4J = 1.5$ Hz, 1 H, H-7), 8.65 (ddd, $^3J = 4.9$, $^4J = 1.5$, $^4J_{\text{PH}} = 0.6$ Hz, 1 H, H-5). $^{13}\text{C}\{^1\text{H}\}$ NMR (D_6 -acetone): $\delta = \text{CMe}_3$ superimposed by solvent signals, 41.66 (d, $^2J = 18.9$ Hz, CMe_3), 126.50 (C-6), 130.57 (d, $^3J = 10.6$ Hz, 2 C-*m*), 131.18 (C-7), 133.00 (d, $^4J = 2.4$ Hz, C-*p*), 134.38 (d, $^2J = 13.5$ Hz, 2 C-*o*), 150.13 (d, $^3J = 13.9$ Hz, C-5), 205.52 (d, $^2J = 8.2$ Hz, 4 *cis*-CO); C_q signals except for *cis*-CO at the noise level. $^{31}\text{P}\{^1\text{H}\}$ NMR (D_6 -acetone): $\delta = 34.9$. IR (KBr): $\nu(\text{CO}) = 2076$ (w), 1944 (vs) cm^{-1} .

DL-(2-*tert*-Butyl-3-isobutyl-1,3-azaphospholo[4,5-*b*]pyridine- $\kappa^1\text{P}$)-pentacarbonyl molybdenum(0) (4c)

$\text{Mo}(\text{CO})_4(\text{NBD})$ (117.1 mg, 0.39 mmol) and **2c** (96.8 mg, 0.39 mmol) were placed into a Schlenk flask, THF (10 mL) was added and the mixture heated at 40 °C for 4 h. Insoluble impurities were filtered off and washed with ether. Removal of the solvent under vacuum provided a yellow-brown oil. ^{31}P NMR monitoring displayed the product ($\delta = 30.6$) along with two contaminants ($\delta = 29.1$, -7.3). Purification by column chromatography on silica gel (hexane/2% ethyl acetate) furnished 61 mg (32%) of an air-sensitive pale yellow viscous oil. $\delta = ^1\text{H}$ NMR (CDCl_3): $\delta = 0.49$ (d, $^3J = 6.4$ Hz, 3 H, CHMe_A), 0.86 (d, $^3J = 6.8$ Hz, 3 H, CHMe_B), 1.54 (s, 9 H, CMe_3), 1.45–1.61 (superimposed m, PCH_2), 2.35 (m, 1 H, CH), 7.38 (ddd, $^3J = 7.9$, 4.9, $^5J_{\text{PH}} = 1.5$ Hz, 1 H, H-6), 7.99 (ddd, $^3J = 7.9$, $^4J_{\text{PH}} = 2.3$, $^4J = 1.5$ Hz, 1 H, H-7), 8.64 (dd, $^3J = 4.9$, $^4J = 1.5$ Hz, 1 H, H-5). $^{13}\text{C}\{^1\text{H}\}$ and DEPT-135 NMR (CDCl_3): $\delta = 23.52$ (d, $^3J = 5.3$ Hz, CMe_A), 24.97 (d, $^3J = 9.3$ Hz, CMe_B), 28.25 (d, $^2J = 8.0$ Hz, CH), 29.86 (d, $^3J = 2.7$ Hz, CMe_3), 39.52 (d, $^1J = 11.9$ Hz, PCH_2), 40.43 (d, $^2J = 18.6$ Hz, CMe_3), 124.68 (s, CH-6), 129.97 (s, CH-7), 147.92 (d, $^2J = 29.2$ Hz, C_q -7a), 148.52 (d, $^3J = 13.3$ Hz, CH-5), 160.05 (d, $^1J = 65.0$ Hz, C_q -3a), 195.25 (d, $^1J = 9.3$ Hz, C_q -2), 204.64 (d, $^2J = 8.9$ Hz, 4 CO_{cis}), 208.94 (d, $^2J = 22.6$ Hz, CO_{trans}). $^{31}\text{P}\{^1\text{H}\}$ NMR (CDCl_3): $\delta = 30.6$. HRMS (DEI): $\text{C}_{19}\text{H}_{21}\text{MoN}_2\text{PO}_5$ (484.29); calcd for $[\text{M}^{98}\text{Mo}]^+$ 486.0237; found 486.0230; calcd for $[\text{M}^{98}\text{Mo}] - \text{CO}]^+$ 458.0287; found: 458.0277.

DL-(2-*tert*-Butyl-3-phenyl-1,3-azaphospholo[4,5-*b*]pyridine- $\kappa^1\text{P}$)-pentacarbonyl tungsten(0) (5a)

A solution of $\text{W}(\text{CO})_5(\text{THF})$, prepared by irradiation of $\text{W}(\text{CO})_6$ (160 mg, 0.455 mmol) in THF (30 mL; 10.2 mL of CO evolved), was added to a solution of **2a** (0.121 g, 0.451 mmol) in THF (5 mL) at -10 °C. Work-up after 2 d as described for **5a** afforded 128 mg (88%) of a pale green powder **5a**, contaminated by a small amount of oligoethylene grease. ^1H NMR (CDCl_3): $\delta = 1.32$ (s, 9 H, CMe_3), 7.38–7.47 (m, 6 H, phenyl, H-6), 8.07 (ddd, $^3J = 8.1$, $^4J_{\text{PH}} = 2.6$, $^4J = 1.5$ Hz, 1 H, H-7), 8.63 (dd, $^3J = 4.8$, $^4J_{\text{PH}} = 1.5$ Hz, 1 H, H-5). $^{13}\text{C}\{^1\text{H}\}$ NMR (CDCl_3): $\delta = 30.25$ (d, $^3J = 2.5$ Hz, CMe_3), 40.98 (d, $^2J = 18.6$ Hz, CMe_3), 125.23 (C-6), 126.03 (d, $^1J = 35.8$ Hz, C_q -i), 129.49 (d, $^3J = 10.6$ Hz, 2 C-*m*), 130.17, 131.91 (2 d, $J = 2.7$ Hz, C-7, C-*p*), 133.48 (d, $^2J = 11.9$ Hz, 2 C-*o*), 148.26 (d, $^2J = 31.8$ Hz, C_q -7a), 149.04 (d, $^3J = 14.6$ Hz, C-5), 162.3 (low int. d, $^1J \approx 75$ Hz,

C_q -3a), 195.41 (d, $^2J = 2.7$ Hz, C_q -2), 195.58 (d, $^2J = 6.6$ Hz, 4 *cis*-CO), 197.23 (d, $^1J = 22.6$ Hz, 1 *trans*-CO). $^{31}\text{P}\{^1\text{H}\}$ NMR (CDCl_3): $\delta = 18.2$ (s, sat, $^1J_{\text{PW}} = 225$ Hz). IR (KBr): $\nu(\text{CO}) = 2075$ (w), 1936 (vs, br) cm^{-1} . MS (EI 70 eV, 80 °C): m/z (%) = 593 (30) $[\text{M}^{184}\text{W}] + \text{H}^+$, 453 (100%) $[\text{M}^{184}\text{W}] + \text{H}^+ - 5 \text{ CO}$. HRMS (ESI in MeCN): calcd for $[\text{M}^{184}\text{W}] + \text{H}^+$ 593.04571; found: 593.04569 (and correct isotopic pattern). Anal. calcd for $\text{C}_{21}\text{H}_{17}\text{N}_2\text{O}_5\text{PW}$ (592.18): H 2.89, N 4.73; found: H 3.15, N 4.67.

DL-(2-*tert*-Butyl-3-phenyl-1,3-azaphospholo[4,5-*b*]pyridine- $\kappa^1\text{P}$)-(η^4 -cycloocta-1,5-diene)rhodium(i)chloride (6a)

$[\text{RhCl}(\text{1,5-COD})]_2$ (32 mg, 0.065 mmol) in THF (5 mL) was added slowly at -20 °C to a solution of **2a** (35 mg, 0.130 mmol) in THF (5 mL). The mixture was stirred overnight at room temperature, resulting in a colour change from yellow to deep orange. Insoluble material was removed by filtration, the solvent was evaporated under vacuum and the residue was washed several times with *n*-hexane and dried under vacuum to give ca. 60 mg (90%) of an orange-yellow solid. ^1H NMR (CDCl_3): $\delta = 1.61$ (s, 9 H, CMe_3), 1.9, 2.4 (vbr s, 8 H, CH_2 , COD), 4.2, 4.6, 5.6 (3 vbr s, 2 H, 1 H, 1 H, =CH, COD), 7.27–7.40 (m, 4 H, H-6, H-*p*, H-*o*), 7.65 (vbr t, $^3J \approx 8.1$ Hz, 2 H, H-*m*), 8.0 (vbr d, $^3J = 7.8$ Hz, 1 H, H-7), 8.45 (vbr, 1 H, H-5). $^{13}\text{C}\{^1\text{H}\}$ and DEPT135 NMR (CDCl_3): $\delta = 30.21$ (superimposed s, CMe_3), 30.8 (superimposed vbr, 4 CH_2 , COD), 41.42 (d, $^2J = 18.4$ Hz, CMe_3), 78.7 (vbr, =CH, COD), 85.8 (vbr, =CH, COD), 105.9 (vbr, 2 =CH, COD), 124.5 (superimposed d, C_q -i), 124.79 (CH-6), 128.80 (d, $^3J = 10.6$ Hz, 2 CH-*m*), 130.4, 131.2 (2 br s, CH-7, CH-*p*), 134.16 (d, $^2J = 12.1$ Hz, 2 CH-*o*), 148.0 (br d, $^3J = 14$ Hz, CH-5), 150.08 (d, $^2J = 27.6$ Hz, C_q -7a), 159.56 (d, $^1J = 68$ Hz, C_q -3a), 192.6 (br, C_q -2). $^{31}\text{P}\{^1\text{H}\}$ NMR (CDCl_3): $\delta = 27.2$ (br d, half width each ≈ 25 Hz, $^1J_{\text{PRh}} = 139$ – 143 Hz), -0.8 (minor solution species, 13–17%). Anal. calcd for $\text{C}_{24}\text{H}_{29}\text{ClN}_2\text{PRh}$ (514.83): C 55.99, H 5.68, N 5.44; found: C 55.58, H 5.43, N 5.35. Orange crystals suitable for XRD analysis, formed by slow diffusion of hexane into a solution of the solid in a small amount of THF, were selected from the mixture with mother liquor. Crystal data are compiled in Table 2, and the selected bond lengths and angles are shown Fig. 1.

DL-(3-*n*-Butyl-2-*tert*-butyl-1,3-azaphospholo[4,5-*b*]pyridine- $\kappa^1\text{P}$)-(η^4 -cycloocta-1,5-diene)rhodium(i)chloride (6b) and detection of 7b

$[\text{RhCl}(\text{1,5-COD})]_2$ (177 mg, 0.36 mmol) in THF (5 mL) was added slowly at -20 °C to a solution of **2b** (178 mg, 0.72 mmol) in THF (10 mL). The mixture was stirred for 1 d at room temperature (colour changed from yellow to deep orange and brownish-yellow) and worked up as described for **6a** yielding 312 mg **6b** (95 mol%, corr. yield 84%) as a yellow powder, containing 5 mol% **7b**. ^1H NMR (CDCl_3): $\delta = 0.77$ (t, $^3J = 7.2$ Hz, 3 H, CH_3), 1.15–1.30 (m, 4 H, CH_2), 1.68 (s, 9 H, CMe_3), 1.79–1.93 (m, 4 H, CH_2 , COD), 2.15–2.40 (m, 2 H, PCH_2), 2.33–2.52 (m, 4 H, CH_2 , COD), 3.67–3.77 (m, 2 H, =CH, COD), 5.50–5.52 (m, $^3J = 3.5$ Hz, 1 H, =CH, COD), 5.6 (vbr s, 1 H,



Table 2 Crystal data and structure refinement

Identification code	6a	9b·2CDCl ₃	10b·4.5THF	10b·2D ₆ -acetone
Empirical formula	C ₂₄ H ₂₉ ClN ₂ PRh	C ₃₆ H ₅₂ D ₂ Cl ₁₀ N ₄ P ₂ Pd ₃	C ₄₆ H ₇₈ Cl ₄ N ₄ O _{4.5} P ₂ Pd ₂	C ₃₄ H ₄₂ D ₁₂ Cl ₄ N ₄ O ₂ P ₂ Pd ₂
Formula weight	514.82	1280.48	1175.66	979.43
Temperature	103(2) K	100(2) K	100(2) K	100(2) K
Wavelength	0.71073 Å	0.71073 Å	0.71073 Å	0.71073 Å
Crystal system	Triclinic	Triclinic	Monoclinic	Monoclinic
Space group	<i>P</i> $\bar{1}$	<i>P</i> $\bar{1}$	<i>C</i> 2/ <i>c</i>	<i>P</i> 2 ₁ / <i>c</i>
Unit cell dimensions	<i>a</i> = 9.1441(6) Å, <i>α</i> = 83.875(2)° <i>b</i> = 9.8885(6) Å, <i>β</i> = 81.588(2)° <i>c</i> = 13.5572(8) Å, <i>γ</i> = 67.831(3)°	<i>a</i> = 8.5594(7) Å, <i>α</i> = 101.959(4)° <i>b</i> = 9.6780(8) Å, <i>β</i> = 92.199(4)° <i>c</i> = 16.4206(13) Å, <i>γ</i> = 109.528(4)°	<i>a</i> = 27.727(3) Å, <i>α</i> = 90° <i>b</i> = 16.625(2) Å, <i>β</i> = 90.891(6)° <i>c</i> = 23.302(3) Å, <i>γ</i> = 90°	<i>a</i> = 11.9584(4) Å, <i>α</i> = 90° <i>b</i> = 29.4872(8) Å, <i>β</i> = 115.816(5)° <i>c</i> = 13.0738(4) Å, <i>γ</i> = 90°
Volume	1121.25(12) Å ³	1245.60(18) Å ³	10 739(2) Å ³	4150.0(2) Å ³
<i>Z</i>	2	1	8	4
Density (calculated)	1.525 Mg m ⁻³	1.707 Mg m ⁻³	1.454 Mg m ⁻³	1.567 Mg m ⁻³
Absorption coefficient	0.965 mm ⁻¹	1.702 mm ⁻¹	0.972 mm ⁻¹	1.236 mm ⁻¹
<i>F</i> (000)	528	636	4864	1968
Crystal size	0.30 × 0.30 × 0.20 mm ³	0.20 × 0.20 × 0.03 mm ³	0.30 × 0.15 × 0.15 mm ³	0.14 × 0.11 × 0.06 mm ³
Theta range for data collection	1.52 to 31.06°	2.30 to 30.58°	2.27 to 30.03°	2.70 to 28.28°
Index ranges	−13 ≤ <i>h</i> ≤ 13, −14 ≤ <i>k</i> ≤ 14, −19 ≤ <i>l</i> ≤ 19	−12 ≤ <i>h</i> ≤ 12, −13 ≤ <i>k</i> ≤ 13, −23 ≤ <i>l</i> ≤ 23	−39 ≤ <i>h</i> ≤ 38, −23 ≤ <i>k</i> ≤ 23, −32 ≤ <i>l</i> ≤ 32	−15 ≤ <i>h</i> ≤ 15, −39 ≤ <i>k</i> ≤ 39, −17 ≤ <i>l</i> ≤ 17
Reflections collected	61 697	38 910	153 859	76 588
Independent reflections	7166 [<i>R</i> (int) = 0.0319]	7630 [<i>R</i> (int) = 0.0307]	15 352 [<i>R</i> (int) = 0.0490]	10 287 [<i>R</i> (int) = 0.0800]
Completeness to theta	= 30.00°, 99.9%	= 30.50°, 100.0%	= 30.00°, 97.7%	= 28.28°, 99.8%
Absorption correction	Semi-empirical from equivalents	Semi-empirical from equivalents	Semi-empirical from equivalents	Semi-empirical from equivalents
Max. and min. transmission	0.830 and 0.694	0.951 and 0.808	0.868 and 0.732	1.000 and 0.952
Refinement method	Full-matrix least-squares on <i>F</i> ²	Full-matrix least-squares on <i>F</i> ²	Full-matrix least-squares on <i>F</i> ²	Full-matrix least-squares on <i>F</i> ²
Data/restraints/parameters	7166/6/281	7630/0/274	15 352/511/585	10 287/266/445
Goodness-of-fit on <i>F</i> ²	1.04	1.03	1.18	0.82
Final <i>R</i> indices [<i>I</i> > 2σ(<i>I</i>)]	<i>R</i> ₁ = 0.0166, w <i>R</i> ₂ = 0.0422	<i>R</i> ₁ = 0.0248, w <i>R</i> ₂ = 0.0572	<i>R</i> ₁ = 0.0409, w <i>R</i> ₂ = 0.0803	<i>R</i> ₁ = 0.0304, w <i>R</i> ₂ = 0.0481
<i>R</i> indices (all data)	<i>R</i> ₁ = 0.0176, w <i>R</i> ₂ = 0.0429	<i>R</i> ₁ = 0.0329, w <i>R</i> ₂ = 0.0612	<i>R</i> ₁ = 0.0782, w <i>R</i> ₂ = 0.0982	<i>R</i> ₁ = 0.0680, w <i>R</i> ₂ = 0.0516
Largest diff. peak and hole	0.52 and −0.32 e Å ⁻³	2.53 and −1.59 e Å ⁻³	1.33 and −0.68 e Å ⁻³	0.76 and −0.47 e Å ⁻³

=CH, COD), 7.37 (ddd, ³*J* = 8.1, 4.9, ⁵*J*_{PH} = 1.6 Hz, 1 H, H-6), 7.93 (ddd, ³*J* = 8.1, ⁴*J*_{PH} = 2.2, ⁴*J* = 1.2 Hz, 1 H, H-7), 8.58 (dd, ³*J* = 4.8, ⁴*J* = 1.2 Hz, 1 H, H-5). ¹³C{¹H} and DEPT135 NMR (CDCl₃): δ = 13.45 (CH₃), 23.25 (d, *J* = 17.5 Hz, CH₂), 23.91 (d, *J* = 13.2 Hz, CH₂), 26.44 (d, *J* = 6.1 Hz, CH₂), 28.60, 28.97 (2 CH₂, COD), 29.77 (*CMe*₃), 32.36 (CH₂, COD), 33.39 (d, *J* = 2.3 Hz, CH₂, COD), 40.96 (d, ²*J* = 18.6 Hz, *CMe*₃), 68.57 (d, *J* = 13.1 Hz, =CH, COD), 72.64 (d, *J* = 13.2 Hz, =CH, COD), 104.73 (dd, *J* = 10.5, 8.1 Hz, =CH, COD), 105.28 (dd, *J* = 12.5, 7.3 Hz, =CH, COD), 124.73 (s, CH-6), 129.85 (d, ³*J* = 2.0 Hz, CH-7), 147.99 (d, ³*J* = 13.2 Hz, CH-5), 150.78 (d, ²*J* = 26.6 Hz, C_q-7a), 156.53 (d, ¹*J* = 67.4 Hz, C_q-3a), 192.29 (d, ¹*J* = 6.1 Hz, C_q-2). ³¹P{¹H} NMR (CDCl₃): δ = 28.2 (d, ¹*J*_{PRh} = 141.7 Hz, 95 mol% **6b**), 17.2 (d, ¹*J*_{PRh} = 151.1 Hz, 5 mol% **7b**). HRMS (ESI in MeCN): calcd for [**6b**-Cl]⁺ 459.1431, calcd. for [**7b**-Cl]⁺ 705.1113; found 459.1431, 705.1111. Anal. calcd for **6b**, C₂₂H₃₃ClN₂PRh (494.84): C 53.40, H 6.72, N 5.66; calcd for **6b/7b** (95/5 mol%): C 52.68, H 6.63, N 5.38; found: C 52.55, H 6.56, N 5.00.

Detection of **8a** and [*meso*-bis{(η³-allyl)(2-*tert*-butyl-3-phenyl-1,3-azaphospholo[4,5-*b*]pyridine-κ¹*P*)palladium(η)chloride}-κ¹*N*]palladium(η)dichloride (**9a**)

Allylpalladium chloride dimer (146 mg, 0.40 mmol) in THF (5 mL) was added slowly at −20 °C to a solution of **2a** (145 mg, 0.54 mmol) in THF (5 mL) and stirred for 2 d at room temperature (colour changed from pale yellow to deep orange). The insoluble material was removed by filtration, the solvent was evaporated under vacuum and the residue was washed several times with *n*-hexane/Et₂O and dried under vacuum to give 202 mg (53% referred to as **2a**, 72% ref. to Pd) of an orange-yellow powder of crude **8a**·THF with CHN analysis values roughly corresponding to a composition [(**2a**){(allyl)-PdCl}_{1.2}(PdCl₂)_{0.8}]_n·C₄H₈O. ¹H NMR (CDCl₃): δ = 1.27 (s, 9 H, *CMe*₃), 2.8 (vbr, 2 H, allyl), 3.5, 5.5, 5.7 (vbr, 3 H, allyl), 7.45 (td, ³*J* ≈ 7.6, ⁴*J* ≈ 1.6 Hz, 2 H, H-*m*), 7.55 (t, ³*J* = 7.8, 7.7 Hz, 1 H, H-*p*), 7.60 (dd, ³*J* = 8.0, 5.8 Hz, 1 H, H-6), 7.9 (vbr s, 2 H, H-*o*), 8.18 (dt, ³*J* = 8.2, ⁴*J* ≈ ⁴*J*_{PH} ≈ 1.5 Hz, 1 H, H-7), 8.8 (vbr,



1 H, H-5); THF: 1.85 (m, 4 H, CH₂), 3.73 (m, 4 H, OCH₂). ¹³C{¹H} and DEPT-135 NMR (CDCl₃): δ = 30.18 (d, ³J = 3.5 Hz, CMe₃), 41.00 (d, ²J = 19.3 Hz, CMe₃), ca. 60 (sh, minor, C'_{allyl}), 62.8 (vbr, C-α_{allyl}), 84.7 (minor, C'_{allyl}), 114.8 (vbr, C_{allyl}), 118.7 (vbr, C_{allyl}), 123.56 (d, ¹J = 31.1 Hz, C_{q-i}), 126.6 (br, CH-6), 129.76 (d, ³J = 10.9 Hz, 2 CH-*m*), 131.46 (s, CH-7), 132.54 (d, ⁴J = 1.9 Hz, CH-*p*), 134.61 (d, ²J = 12.1 Hz, 2 CH-*o*), 150.26 (d, ²J = 27.2 Hz, C_{q-7a}), 151.5 (vbr, CH-5), 160 (br d, ¹J ≈ 60 Hz, C_{q-3a}), 195.4 (br, C_{q-2}); THF 25.60 (CH₂), 67.96 (OCH₂). ³¹P{¹H} NMR (CDCl₃): δ = 15.4 (vbr). Anal. calcd for **8a**-THF (C₂₃H₃₀Cl₃N₂OPd₂, 700.67): C 39.43, H 4.32, N 4.00; calcd for [(**2a**)(allylPdCl)_{1.2}(PdCl₂)_{0.8}]-C₄H₈O (C_{23.6}H₃₁Cl_{2.8}N₂OPd₂, 701.80): C 40.39, H 4.45, N 3.99; found: C 40.66, H 4.18, N 3.54. Slow diffusion of hexane into a concentrated solution of crude **8a** in THF gave crystals of **9a**-THF. Severe disorder of the allyl group and unexpected peaks in the residual electron density (possibly by twinning) did not allow satisfactory refinement of the XRD data, but allowed the identification of **9a**-THF (Fig. S26, ESI†).

[meso-Bis{(η³-allyl)(3-*n*-butyl-2-*tert*-butyl-1,3-azaphospholo[4,5-*b*]pyridine-κ¹P)palladium(II)chloride}-κ¹N]palladium(II)dichloride (9b**)**

Reaction of allylpalladium chloride dimer (180 mg, 0.49 mmol) in THF (10 mL) with **2b** (0.162 g, 0.652 mmol) in THF (15 mL) and workup as described for **8a** gave 250 mg (74%) yellow powder. CHN analysis values are in accordance with THF-free **9b**. Crude powder with residual THF – ¹H NMR (CDCl₃): δ = 0.80 (t, ³J = 7.2 Hz, 3 H, CH₃), 1.28 (m, ³J = 7.8, 6.8 Hz, 4 H, CH₂), 1.47 (br s, 9 H, CMe₃), 2.6 (vbr s, 2 H, PCH₂ and/or allyl), 2.7–3.4 (vbr m, 2 H, allyl and/or PCH₂), 3.55–3.9 (superimposed by THF, vbr, H_{allyl}), 4.0–4.2 (vbr, H_{allyl}), 4.8, 5.3–5.8 (vbr, H_{allyl}), 7.5 (vbr, 1 H, H-6), 8.1 (vbr d, ³J ≈ 7 Hz, 1 H, H-7), 8.7 (vbr, 1 H, H-5); ca. 0.3 THF/**9b**: 1.85 (m, CH₂), 3.75 (m, OCH₂). ¹³C{¹H} NMR (CDCl₃): δ = 13.43 (s, CH₃), 23.6–23.8 (br superimposed d, 2 CH₂), 26.53 (d, *J* = 8.2 Hz, CH₂), 29.68 (d, ³J = 2.9 Hz, CMe₃), 40.54 (d, ²J = 19.6 Hz, CMe₃), 58 (vbr, C'_{α-allyl}), 62.2 (vbr, C-α_{allyl}), 80.5 (vbr, C-γ_{allyl}), 114.6 (br, C-β'_{allyl}), 117.2, 118.8 (vbr, C-β_{allyl}), 125.3 (vbr, C-6), 130.5 (vbr, C-7), 148.5–150.5 (vbr, C-5, C_{q-7a}), 158.6 (br d, ¹J ≈ 72 Hz, C_{q-3a}), 192.4 (br, low int., C_{q-2}); int. C_{all}: C'_{all} ca. 3 : 1. ³¹P{¹H} NMR (CDCl₃): δ = 17 (vbr), 25 (vbr), integral ratio 3 : 1. Anal. calcd for C₃₄H₅₂Cl₄N₄P₂Pd₃ (1039.82): C 39.27, H 5.04, N 5.39; found: C 38.87, H 5.12, N 5.14. Single crystals of **9b**-2CDCl₃, grown by slow concentration of the CDCl₃ solution, were selected from the mixture with mother liquor for crystal structure determination. For selected bond lengths and angles see Fig. 3, and for crystal data see Table 2.

DL-anti-Bis{[(3-*n*-butyl-2-*tert*-butyl-1,3-azaphospholo[4,5-*b*]pyridine)-κ¹N,κ¹P]cis-palladium(II)dichloride} (10b**) solvates**

(A) **10b**-4.5THF. [Pd(CH₃CN)₂Cl₂] (96.5 mg, 0.372 mmol) in THF (10 mL) was added slowly at –10 °C to a solution of **2b** (92.4 mg, 0.372 mmol) in THF (10 mL). The reaction mixture was stirred for 2 d at room temperature (colour changed from pale yellow to orange) and filtered. Removal of the solvent under vacuum, washing the orange solid residue with

n-hexane and drying under vacuum gave 120 mg (76%) yellow powder. ¹H NMR (CDCl₃): δ = 0.77 (t, ³J = 7.2 Hz, 3 H, CH₃), 0.70–0.95 (superimposed m, 2 H, CH₂), 1.13–1.28 (m, 2 H, CH₂), 1.57 (s, 9 H, CMe₃), 2.32–2.47 (m, 1 H, PCH), 3.67–3.84 (m, 1 H, PCH), 7.45 (ddt, ³J ≈ 8, 5, |⁵J_{PH} + ⁵J_{PH}| = 3.5 Hz, 1 H, H-6), 7.94 (dt, ³J = 8.1, ⁴J_{PH} = 2, ⁴J = 1.2 Hz, 1 H, H-7), 8.54 (tt, |³J + ⁴J_{PH}| = 4.2, ⁴J ≈ ⁴J_{PH} = 1.2, 1.4 Hz, 1 H, H-5). ¹³C{¹H} NMR (CDCl₃): δ = 13.48 (s, CH₃), 23.50 (d, *J* = 14.1 Hz, CH₂), 24.79 (d, *J* = 17.4 Hz, CH₂), 25.39 (d, *J* = 10.1 Hz, CH₂), 29.74 (d, ³J = 3.8 Hz, CMe₃), 40.70 (d, ²J = 21.1 Hz, CMe₃), 127.59 (CH-6), 132.36 (CH-7), 150.6 (superimposed d, ³J = 10 Hz, CH-5), 150.7 (superimposed d, ²J = 28 Hz, C_{q-7a}), 157.3 (partly at noise level, C_{q-3a}), 190.4 (br, C_{q-2}). ³¹P{¹H} NMR (CDCl₃): δ = 26.7. Anal. calcd for THF free complex C₂₈H₄₂Cl₄N₄P₂Pd₂ (851.26): C 39.51, H 4.97, N 6.58; found: C (incomplete combustion), H 5.25, N 6.73. Single crystals of **10b**-4.5THF were obtained by slow diffusion of *n*-hexane into the saturated solution in THF; the solvent was lost rapidly in air, and the crystal had to be handled under inert oil. Crystal data are given in Table 2, and the selected bond lengths and angles in Fig. 4a.

(B) **10b**-2D₆-acetone. K₂PdCl₄ (120 mg, 0.368 mmol) in MeOH (10 mL) was added slowly at –20 °C to a solution of **2b** (89 mg, 0.358 mmol) in MeOH (10 mL). The mixture was stirred for 3 d at room temperature, filtered, and the deep yellow precipitate was washed several times with water and MeOH, and then dried under vacuum yielding 108 mg (71%) of a yellow air-stable powder. This was insoluble in *n*-hexane and slightly soluble in acetone. ¹H NMR (D₆-acetone): δ = 0.75 (t, ³J = 7.3 Hz, 3 H, CH₃), 1.0–1.43 (m, 4 H, CH₂), 1.82 (s, 9 H, CMe₃), 3.2–3.35, 3.7–3.85 (vbr m, 2 H, PCH), 7.69 (ddd, ³J = 8.2, 5.7, ⁵J_{PH} = 1.4 Hz, 1 H, H-6), 8.08 (dt, ³J = 8.2, ⁴J ≈ ⁴J_{PH} = 1.2 Hz, 1 H, H-7), 8.40 (dt, ³J = 5.6, ⁴J ≈ ⁴J_{PH} = 1 Hz, 1 H, 5-H). ¹³C{¹H} NMR (D₆-acetone): δ = 14.26 (CH₃), 24.64 (d, *J* = 16.6 Hz, CH₂), 25.59 (d, *J* = 22.6 Hz, CH₂), 26.96 (d, *J* = 20.4 Hz, CH₂), 29 (br s superimposed with solvent, CMe₃), 43.23 (d, ²J = 20.4 Hz, CMe₃), 131.3 (vbr, CH-6), 135.2 (vbr, CH-7), 152.5 (vbr, CH-5); C_q-signals in noise. ³¹P{¹H} NMR (D₆-acetone): δ = 31.0. LRMS (ESI in MeCN): calcd for most abundant fragment [M – Cl]⁺ 815.00; found: 815.00 (and correct isotopic pattern). Anal. calcd for C₂₈H₄₂Cl₄N₄P₂Pd₂ (851.26): C 39.51, H 4.97, N 6.58; found: C 40.06, H 5.06, N 6.34. Slow diffusion of *n*-hexane into a saturated solution in D₆-acetone provided single crystals of **10b**-2D₆-acetone. Crystal data are given in Table 2, and the structure is shown in Fig. 4b.

Catalytic tests – 2-mesitylamino pyridine 11

A Schlenk bottle was charged with 2-bromopyridine (212 mg, 1.34 mmol), mesitylamine (269 mg, 1.99 mmol), KO^tBu (310 mg, 2.76 mmol), **10b** (prepared from Pd(CH₃CN)₂Cl₂, 29 mg) or the given amount of ligand and Pd-compound (see Table 1) and toluene (10 mL) and heated under nitrogen for 24 h at 100 °C. The mixture was filtered, washed with toluene, the solution was transferred to a silica gel column and compound **11** was separated using ethyl acetate/hexane 2 : 8. The results are compiled in Table 1. The ¹H and ¹³C NMR data of **11** were in accordance with known values.²²



Crystal structure analysis

Crystals of **6a**, **9b**·2CDCl₃, **10b**·2D₆-acetone and **10b**·4.5THF were mounted on glass fibres in an inert oil. Data were recorded at low temperature on an Oxford Diffraction Xcalibur E (**10b**·2(D₆-acetone)) or a Bruker APEX2 diffractometer using MoK α -radiation ($\lambda = 0.71073 \text{ \AA}$). Crystal data are summarized in Table 2. The structures were refined anisotropically on F^2 using the program SHELXL-97.²⁶ Hydrogen atoms were included using a riding model or rigid methyl groups, except for hydrogens of coordinated allyls or coordinated double bonds, which were refined freely. For **10b**·4.5THF, one THF is disordered over two positions and one lies on a twofold axis.

Crystallographic data for **6a**, **9b**·2CDCl₃, **10b**·4.5THF and **10b**·2D₆-acetone have been deposited with the Cambridge Crystallographic Data Centre as supplementary publication no. CCDC 1423102, 1423105, 1423103 and 1423104 respectively.

Acknowledgements

A fellowship (M.S.S.A.) from the Deutscher Akademischer Austauschdienst (DAAD) and financial support by the Deutsche Forschungsgemeinschaft (HE 1997/12-2) are gratefully acknowledged. We thank B. Witt, G. Thede and M. Steinich for NMR and LRMS and Dr H. Frauendorf and G. Sommer-Udvarnoki (Georg-August-Universität Göttingen, Institut für Organische und Biomolekulare Chemie) for HRMS measurements.

References

- (a) G. R. Newkome, *Chem. Rev.*, 1993, **93**, 2067–2089; (b) Z. Z. Zhang and H. Cheng, *Coord. Chem. Rev.*, 1996, **147**, 1–39; (c) P. Espinet and K. Soulantica, *Coord. Chem. Rev.*, 1999, **193–195**, 499–556.
- (a) M. M. Olmstead, A. Maisonnat, J. P. Farr and A. L. Balch, *Inorg. Chem.*, 1981, **20**, 4060–4064; (b) J. P. Farr, M. M. Olmstead, F. Wood and A. L. Balch, *J. Am. Chem. Soc.*, 1983, **105**, 792–798; (c) A. Ecke, W. Keim, M. C. Bonnet, I. Tkatchenko and F. Dahan, *Organometallics*, 1995, **14**, 5302–5307.
- S. Durben and T. Baumgartner, *Inorg. Chem.*, 2011, **50**, 6823–6836.
- (a) M. S. S. Adam, O. Köhl, M. K. Kindermann, J. W. Heinicke and P. G. Jones, *Tetrahedron*, 2008, **64**, 7960–7967; (b) M. S. S. Adam, P. G. Jones and J. W. Heinicke, *Eur. J. Inorg. Chem.*, 2010, 3307–3316.
- (a) R. K. Bansal and J. Heinicke, *Chem. Rev.*, 2001, **101**, 3549–3578; (b) J. Heinicke, N. Gupta, S. Singh, A. Surana, O. Köhl, R. K. Bansal, K. Karaghiosoff and M. Vogt, *Z. Anorg. Allg. Chem.*, 2002, **628**, 2869–2876; (c) J. Heinicke, K. Steinhäuser, N. Peulecke, A. Spannenberg, P. Mayer and K. Karaghiosoff, *Organometallics*, 2002, **21**, 912–919; (d) M. Ghalib, B. Niaz, P. G. Jones and J. W. Heinicke, *Heteroat. Chem.*, 2013, **24**, 452–456.
- (a) M. Ghalib, L. Könczöl, L. Nyulászi, P. G. Jones, G. J. Palm and J. W. Heinicke, *Dalton Trans.*, 2014, **43**, 51–54; (b) M. Ghalib, L. Könczöl, L. Nyulászi, G. J. Palm, C. Schulzke and J. W. Heinicke, *Dalton Trans.*, 2015, **44**, 1769–1774; (c) M. Ghalib, P. G. Jones, C. Schulzke, D. Sziebert, L. Nyulászi and J. W. Heinicke, *Inorg. Chem.*, 2015, 2117–2127; (d) J. Heinicke, *Eur. J. Inorg. Chem.*, 2016, DOI: 10.1002/ejic.201500941.
- (a) S. O. Grim, D. A. Wheatland and W. McFarlane, *J. Am. Chem. Soc.*, 1967, **89**, 5573–5577; (b) F. A. Cotton and C. S. Kraihanzel, *J. Am. Chem. Soc.*, 1962, 4432–4438.
- (a) E. O. Fischer, L. Knauss, R. L. Keiter and J. G. Verkade, *J. Organomet. Chem.*, 1972, **37**, C7–C10; (b) F. Mercier, F. Mathey, C. Afiong-Akpan and J. F. Nixon, *J. Organomet. Chem.*, 1988, **348**, 361–367.
- (a) M. A. M. Meester, R. C. J. Vriends, D. J. Stufkens and K. Vrieze, *Inorg. Chim. Acta*, 1976, **19**, 95–103; (b) H. Daamen and A. Oskam, *Inorg. Chim. Acta*, 1978, **26**, 81–89.
- W. Partenheimer and E. F. Hoy, *Inorg. Chem.*, 1973, **12**, 2805–2809.
- E. Rotondo, G. Battaglia, C. G. Arena and F. Faraone, *J. Organomet. Chem.*, 1991, **419**, 399–402.
- (a) J. Tiburcio, S. Bernes and H. Torrens, *Polyhedron*, 2006, **25**, 1549–1554; (b) K. Vrieze, H. C. Volger and A. P. Praat, *J. Organomet. Chem.*, 1968, **14**, 185–200.
- (a) H. L. M. van Gaal and J. P. J. Verlaan, *J. Organomet. Chem.*, 1977, **133**, 93–106; (b) I. J. Colquhoun and W. McFarlane, *J. Magn. Reson.*, 1982, **46**, 525–528.
- (a) B. R. Aluri, M. K. Kindermann, P. G. Jones and J. W. Heinicke, *Chem. – Eur. J.*, 2008, **14**, 4328–4335; (b) M. Ghalib, P. G. Jones, S. Lysenko and J. W. Heinicke, *Organometallics*, 2014, **33**, 804–816.
- A. Brück and K. Ruhland, *Organometallics*, 2009, **28**, 6383–6401.
- S. Chen, E. Manoury and R. Poli, *Eur. J. Inorg. Chem.*, 2014, 5820–5826.
- J. Rajput, A. T. Hutton, J. R. Moss, H. Su and C. Imrie, *J. Organomet. Chem.*, 2006, **691**, 4573–4588.
- L. Bettucci, C. Bianchini, J. Filippi, A. Lavacchi and W. Oberhauser, *Eur. J. Inorg. Chem.*, 2011, 1797–1805.
- B. Henc, P. W. Jolly, R. Salz, G. Wilke, R. Benn, E. G. Hoffmann, R. Mynott, G. Schroth, K. Seevogel, J. C. Sekutowski and C. Krüger, *J. Organomet. Chem.*, 1980, **191**, 425–448.
- B. E. Mann, R. Pietropaolo and B. L. Shaw, *J. Chem. Soc., Dalton Trans.*, 1973, 2390–2393.
- P. Braunstein and F. Naud, *Angew. Chem., Int. Ed.*, 2001, **40**, 680–699.
- E. J. Crust, I. J. Munslow, C. Morton and P. Scott, *Dalton Trans.*, 2004, 2257–2266.
- M. S. S. Adam, A. D. Mohamad, P. G. Jones, M. K. Kindermann and J. W. Heinicke, *Polyhedron*, 2013, **50**, 101–111.
- (a) J. P. Wolfe, S. Wagaw, J.-F. Marcoux and S. L. Buchwald, *Acc. Chem. Res.*, 1998, **31**, 805–818; (b) J. F. Hartwig, *Acc. Chem. Res.*, 1998, **31**, 853–860.
- T. H. Riermeier, A. Zapf and M. Beller, *Top. Catal.*, 1997, **4**, 301–309.
- G. M. Sheldrick, *Acta Crystallogr., Sect. A: Fundam. Crystallogr.*, 2008, **64**, 112–122.

